Contribution from the Department of Chemistry, University of the Western Cape, Bellville 7530, South Africa, and Laboratorium für Chemische und Mineralogische Kristallographie, Universität Bern, Freiestrasse 3, CH-3012 Bern, Switzerland

Molecular Geometry of d^8 Five-Coordination. 1. Data Search, Description of Conformation, and Preliminary Statistics

Thomas P. E. Auf der Heyde*,† and Hans-Beat Bürgi‡

Received November 28, 1988

In this paper, the first of a three-part series, the search for and subsequent withdrawal of crystallographic data on a total of 196 five-coordinate d^8 metal complexes are outlined. For each ML_5 molecular fragment (M = Ni(II), Pd(II), Pt(II), Rh(I), Ir(I); L = coordinated ligand atom), the geometry has been precisely described by two sets of 12 nonredundant symmetry coordinates. These sets correspond to the two most common idealized five-coordinate conformations: the trigonal bipyramid (TBP) of D_{3h} symmetry and the square-based (or rectangular) pyramid (SQP) of C_{4v} symmetry. Each observed ML_5 fragment is considered to be represented by a point in a 12-dimensional space spanned by the symmetry coordinates. There are two such spaces, depending on whether the observed structures are related to a TBP (T-space) or a SQP (S-space). T-space consists of 12 asymmetric units related to each other by the symmetry of the D_{3h} point group, while S-space contains 8 asymmetric units whose relations to each other are determined by the symmetry of the C_{4v} point group. In order to take into account these symmetries, each representative point in the two data spaces is transformed into its 12 or 8 isometric partners, respectively, by the application of the symmetry operations of the respective point groups. This amounts to an expansion of the data set by a factor of 12 in the case of T-space and a factor of 8 in that of S-space, resulting in a total of 2352 and 1568 data points, respectively. "Standard" M–L bond lengths are derived by using Pauling's empirical bond length–bond strength relationship, in order to express observed M–L interatomic distances as increments of the standard distances. Interatomic angles are approximately scaled to the dimensions of the distance increments by expressing them in radians as angular displacements along the circumference of a circle whose radius equals the average M–L distance in the data set. Univariate statistics reveal that the variance in the equatorial bonds of the TBP is greater than that of the axial ones and that one equatorial angle is inversely related to the other two. For the SQP, the apical bond exhibits much greater variance than either of the four basal bonds, while the trans-basal angles have the most significant angular variation. Bivariate statistics suggest distortions reminiscent of classical S_N2 and Berry intramolecular exchange coordinates in the TBP, as well as one that indicates the preservation of a constant amount of bond order at the metal (the "glue" coordinate). The SQP distorts along the glue coordinate and along one delineating the pyramidalization of the pyramid. The sum of these is akin to an addition/elimination coordinate for the addition of a fifth ligand to a square-planar ML_4 complex.

Introduction

Five-coordinate intermediates and/or transition states have been postulated and demonstrated for many ligand exchange reactions of square-planar molecules. These have historically been divided into three main groups—nucleophilic substitutions, electrophilic substitutions, and oxidative additions followed by reductive eliminations. It is becoming increasingly clear, however, that a relationship exists between many types of reaction mechanisms previously classified quite separately.[1-3] Often this relationship results from *geometrically similar* reaction pathways involving the formation of a five-coordinate species, be it a true intermediate in an associative nucleophilic substitution, an early transition state in an oxidative addition, or a solvento species in a dissociative electrophilic substitution, for example. In this sense then, many, if not most, reactions of four-coordinate complexes can be deemed at some stage to involve the formation of a five-coordinate species

$$XML_3 + Y \rightleftharpoons [XML_3Y] \rightleftharpoons X + ML_3Y$$

where X and L represent any ligand atom and Y is either X, L, or solvent. There is general agreement that this reaction involves attack (nucleophilic or electrophilic) at the metal by the incoming "ligand" Y, with the five-coordinate intermediate adopting trigonal-bipyramidal and square-pyramidal conformations at various stages along the reaction pathway. In most cases, though, geometrical details concerning conformational changes along the reaction have not been forthcoming. Cross[1-3] has reviewed the published work in this area with particular attention to the geometrical implications of the studied reactions,[2] but most of his conclusions have had to remain speculative in this regard, due to the classic difficulty of direct observation of the reacting species.

Lack of a suitable technique for direct observation of the reacting species has always plagued investigations into the dynamics of reacting chemical systems; the precise geometrical changes taking place along the reaction pathway are usually elusive. For simple systems containing, e.g., five atoms not heavier than fluorine, this problem can sometimes be overcome by ab initio calculations of the Born–Oppenheimer potential energy surface for the chemical system. For the type of reaction referred to earlier, however, it seems extremely unlikely that potential energy surfaces derived from ab initio theory will be used for the routine examination of reaction pathways in the near future.[4]

Although direct *observation* of a molecule along the reaction pathway does not seem feasible, its *visualization* at least does. According to the structure correlation hypothesis,[5] the *gradual* distortion or *static deformation* that a molecular fragment of interest manifests *collectively* over a large variety of crystalline frameworks may be assumed to mirror the distortion which that fragment would undergo along a given reaction coordinate. The various crystals or molecular structures are considered to constitute a series of "frozen-in" points, or snapshots, taken along the reaction pathway, which, when viewed in the correct order, yield a cinematic film of the reaction.

The rationale behind the hypothesis is enticingly simple and insightful. Crystalline structures represent stable atomic arrangements—their representative points on the potential energy surface will consequently lie in, or close to, a local potential minimum, either a "well", a "dip", or a point in a "valley". Crystal structures containing closely related molecular fragments will be represented by points variously displaced from the potential minima, *along pathways of minimum energy*. Arranged in the correct sequence, then, these fragments can be assumed to map such pathways, their static deformation mirroring that expected along the coordinate. This idea has found expression in the structure correlation hypothesis: *If a correlation can be found between two or more independent parameters describing the structure of a given structural fragment in a variety of environments, then the correlation function maps a minimum energy path in the corresponding parameter space.*[5c] The structure correlation method has been used to map reaction paths for a

* To whom correspondence should be addressed.
† University of the Western Cape.
‡ Universität Bern.

(1) Anderson, G. K.; Cross, R. J. *Acc. Chem. Res.* **1984**, *17*, 67–74.
(2) Cross, R. J. *Chem. Soc. Rev.* **1985**, *14*, 197–223.
(3) Cross, R. J. *Mechanisms of Inorganic and Organometallic Reactions*; Plenum Press: New York, 1984; Vol. 2, Chapter 5.
(4) Truhlar, D. G.; Steckler, R.; Gordon, M. S. *Chem. Rev.* **1987**, *87*, 217–236.
(5) (a) Bürgi, H.-B. *Inorg. Chem.* **1973**, *12*, 2321–2325. (b) Bürgi, H.-B.; Dunitz, J. D. *Acc. Chem. Res.* **1983**, *16*, 153–161. (c) Murray-Rust, P.; Bürgi, H.-B.; Dunitz, J. D. *J. Am. Chem. Soc.* **1975**, *97*, 921–922.

0020-1669/89/1328-3960$01.50/0

Table I. Definition of Angular Range (deg) for a Typical Five-Coordinate Fragment[a]

	θ_{12}	θ_{13}	θ_{14}	θ_{23}	θ_{24}	θ_{34}	θ_{25}	θ_{35}	θ_{45}	θ_{15}
TBP	90	90	90	120	120	120	90	90	90	180
SQP	86	105	86	105	150	105	86	105	86	150
range	75–108	80–110	75–108	70–132	105–175	70–132	66–107	66–108	66–107	150–180

[a] Angles θ_{ij} refer to angles between atoms i and j according to the labeling scheme shown in Figure 1, i.e., a TBP with axial ligands 1 and 5 and a SQP with apical ligand 3 and transbasal ligand pairs 1 and 5, and 2 and 4.

variety of different reactions, including substitution and addition reactions, dissociations, conformational interconversions, and isomerizations.[6] In many cases, the reaction coordinates closely parallel those derived from theoretical calculations, both ab initio and semiempirical.[7,8]

This study examines in detail the molecular geometry of 196 five-coordinate structures, each containing a metal center with a d^8 electron configuration—either nickel(II), palladium(II), platinum(II), rhodium(I), or iridium(I). The investigation will go beyond the simple use of two-dimensional methods of data analysis such as scatter plots or correlation coefficients, since a complete description of the geometry of a six-atom fragment necessitates 12 geometrically independent parameters. Each five-coordinate molecular fragment will hence be considered in terms of its representative point in a 12-dimensional space spanned by a set of 12 geometric parameters. Multivariate statistical techniques capable of analyzing hyperspaces are then used as tools in order to explore the data distribution in this space: the presence of clusters of data points will be investigated by cluster analysis, while the shapes of the overall distribution and of the clusters will be characterized by factor analysis. The averaged or archetypal geometries representing the cluster centers and their static deformations, derived from the distortions and elongations of the clusters, will then be discussed in the light of the structure correlation hypothesis to establish the relationship between the static deformations mapped by the five-coordinate molecular fragments and reaction coordinates of five-coordinate complexes. During the analysis, comparisons will be made to the results of our earlier study of the dynamic stereochemistry of nickel,[9] which was based largely on the interpretation of two-dimensional scatter plots.

The results of this study will be presented in three parts. Part 1 deals with the data search and retrieval, the description of the molecular geometry, and preparation of the data for the statistical analysis, and it reports and briefly discusses univariate and bivariate statistics. Part 2[10] reports the results of cluster analysis and discusses the implications of these results, while Part 3[10] deals with the results of factor analysis and their implications, summarizes the overall picture, and discusses it in the context of the structure correlation hypothesis and of the underlying chemistry.

Experimental Section

1. Data Search. The Crystallographic Data Centre of Cambridge University maintains a set of computer files that contains a database relating to the structures of organic and organometallic compounds and metal complexes as determined by X-ray or neutron diffraction.[11] This database will hereinafter be referred to as the Cambridge Structural Database (CSD). The choice of fragment for which the CSD is to be searched needs to be a judicious compromise between a definition that is too narrow in its scope, thus precluding the retrieval of entries whose particular distortions might be of extreme interest and importance and one that is so broadly stated as to include fragments or data which add nothing to the analysis—apart, that is, from effort and time spent on it.

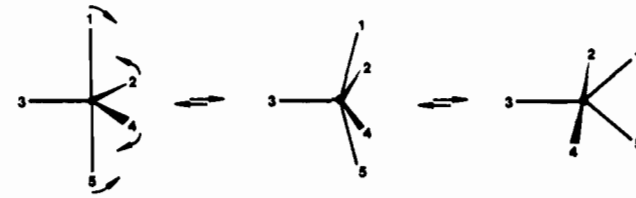

Figure 1. Diagram showing the Berry mechanism and ligand numbering schemes for TBP (left) and SQP (center).

(a) Fragment Definition. In attempting to examine the molecular conformation of d^8 five-coordinate metal complexes the question must be asked: What is a five-coordinate compound? The answer is not as straightforward or as simple as it may at first seem. It has by now been well established that for certain metal complexes there is a relatively smooth progression from a tetracoordinate to a pentacoordinate state and, in some cases, from the latter to a hexacoordinate state. Bürgi has shown that this is the case for cadmium,[5a] Britton and Dunitz have shown this for tin, germanium, and lead,[12] and we have shown it for zinc[7] and nickel[9a]—to name but a few. Consequently, the choice of whether a given metal complex is to be labeled as "four-coordinate", "five-coordinate", or "six-coordinate" is sometimes made on the basis of subjective criteria depending on whether an author of a paper is looking for (or expecting) one coordination number rather than another. Unfortunately, though, when such a case is included in the CSD, the author's possibly subjective evaluation or prejudice is simultaneously included in the data.

Obviously this complicates the search for appropriate fragments, since it is precisely those fragments on the borderline between the two coordination numbers that offer unique insights—according to the structure correlation hypothesis they map out the pathway for the addition of a fifth ligand to a four-coordinate metal center. (We will hereinafter refer to such compounds as "four-plus-one" coordinate.) Clearly the inclusion of four-coordinate entries that happen to have a fifth atom in some proximity to the metal would be appropriate only for compounds for which it can somehow be verified that the extra atom is there by virtue of some interaction with the metal center, rather than as a trivial consequence of its attachment to one of the four other ligands.

In light of these considerations, we decided on a two-pronged approach to the problem of data retrieval. First, those entries listed as five-coordinate in the CSD for nickel, palladium, platinum, rhodium, and iridium were to be withdrawn. Second, all entries for these metals listed as four-coordinate would be withdrawn and then subsequently searched for fragments that might alternatively be classified as five-coordinate or as "approaching five-coordination", i.e., the four-plus-one coordinate entries.

In order to effect the latter search, some a priori concept of a fragment fitting the general description of "five-coordinate" had to be developed. To begin with, we decided to limit the distance between the central metal and its five ligand donor atoms to no more than 3.4 Å. It has been found[7,9,12,13] that distances of this order represent the maximum at which an interatomic interaction of sorts can reasonably be postulated, this distance in most cases being larger than the sum of the van der Waals radii. Clearly, one could have included fragments with interatomic distances greater than this, but experience has shown that the statistical scatter becomes totally random beyond this point.[13]

In addition, given our experience gathered during previous studies,[7,9a] a five-coordinate fragment was defined on the basis of bond angles contained within it. By far the most commonly adopted conformations among pentacoordinate main-group and transition-element complexes are

(6) We will not give a full review of these here. For this, the reader is referred to ref 5b and 9.
(7) Auf der Heyde, T. P. E.; Nassimbeni, L. R. *Acta Crystallogr.* **1984**, *B40*, 582–590.
(8) (a) Bürgi, H.-B.;Lehn, J. M.; Wipff, G. *J. Am. Chem. Soc.* **1974**, *96*, 1956–1957. (b) Klebe, G. *J. Organomet. Chem.* **1987**, *332*, 35–46. (c) Gilli, G.; Bertolasi, V.; Bellucci, F.; Ferretti, V. *J. Am. Chem. Soc.* **1986**, *108*, 2420–2424.
(9) (a) Auf der Heyde, T. P. E.; Nassimbeni, L. R. *Inorg. Chem.* **1984**, *23*, 4525–4532. (b) Auf der Heyde, T. P. E. M.Sc. Dissertation, University of Cape Town, 1984.
(10) See: Auf der Heyde, T. P. E.; Bürgi, H.-B. *Inorg. Chem.*, following two papers in this issue.
(11) Allen, F. H.; Bellard, S.; Brice, M. D.; Cartwright, B. A.; Doubleday, A.; Higgs, H.; Hummelink, T.; Hummelink-Peters, B. G.; Kennard, O.; Motherwell, W. D. S.; Rodgers, J. R.; Watson, D. G. *Acta Crystallogr.* **1979**, *B35*, 2331–2339.
(12) Britton, D.; Dunitz, J. D. *J. Am. Chem. Soc.* **1981**, *103*, 2971–2979.
(13) (a) Rosenfield, R. E., Jr.; Murray-Rust, P. *J. Am. Chem. Soc.* **1982**, *104*, 5427–5430. (b) Rosenfield, R. E., Jr.; Parthasarathy, R.; Dunitz, J. D. *J. Am. Chem. Soc.* **1977**, *99*, 4860–4862. (c) Guru Row, T. N.; Parthasarathy, R. *J. Am. Chem. Soc.* **1981**, *103*, 477–479.

the trigonal bipyramid (TBP) and the square-based (or rectangular) pyramid (SQP), or slightly distorted forms of either. Indeed, it is now well established that the TBP and the SQP are readily interconvertible via the Berry mechanism.[14] This involves simultaneous in-plane bends of the axial ligands (atoms 1 and 5 in Figure 1) and two of the equatorial ligands (atoms 2 and 4), with the third equatorial ligand (atom 3) acting as a "pivot" for what has (inappropriately) been called a pseudorotation mechanism. When these in-plane bends are continued beyond the SQP level a new TBP is formed as shown in Figure 1.

Thus, the primary types of distortions away from idealized trigonal-bipyramidal or square-based-pyramidal conformation which are observed among pentacoordinate complexes are distortions "along" the Berry coordinate. These include mainly a reduction in the angle between the axial ligands (θ_{15}) with a concomitant opening of that between two equatorial ligands (θ_{24}) in the TBP or, conversely, a widening of one trans-basal angle (θ_{15}) and a reduction of the other (θ_{24}) in the SQP. Over the last 2 decades, in particular, these general distortions have been well documented for both main-group and transition-element complexes, and Holmes has recently written a comprehensive review of the area.[15]

These considerations led to the "angular" definition of a five-coordinate molecular fragment as indicated in Table I. Included also in this table are the intrafragment angles as defined for the TBP and one example (of many possible ones) of these angles for an "ideal" SQP. The values for the SQP have been used by Holmes[15] as well as by us in our earlier studies,[7,9a] and they are obtained by placing M at the center of mass of a $[L_5]$ square pyramid, with the distances from the central M to the five L atoms all equal. They are listed here merely for the purpose of comparison with the ranges defined by us for this study, since it has been suggested that the values of the intrafragment angles of a SQP will depend on the d-orbital electron configuration.[16-18]

(b) Data Retrieval. Identification of Five-Coordinate Entries. A search of the July 1984 version of the CSD, at that stage containing 42 381 entries, revealed 124 compounds containing nickel in an exactly five-coordinate environment, as well as 11 palladium, 17 platinum, 50 rhodium, and 59 iridium entries. These "hits" were then manually sorted, rejecting those listed without atomic coordinates, those with disordered structures, allyl compounds, those with an error flag, and compounds whose coordination number was incorrect or whose oxidation state, as judged by the entry in the CSD, precluded a d^8 electron configuration. Allyl complexes were rejected on the basis that a definite atom or point of ligation of the allyl ligand would be difficult to identify. During this sorting procedure 27 nickel, 6 palladium, 9 platinum, 28 rhodium, and 34 iridium entries were rejected.

In order to test the angular definition of a five-coordinate fragment (as set out in Table I), we used the data set of known five-coordinate compounds for a test run. The key words and parameters for the program GEOM (implemented in the CSD) are shown in Table II.

Essentially, the program numbered the ligands in such a way as to restrict the values of the interatomic angles found in the fragment to the ranges set out in Table I. In other words, it attempted to superimpose onto the pentacoordinate molecular fragments the ligand numbering scheme employed in Figure 1 and Table I, according to which a distortion away from a TBP toward a SQP manifests itself through a reduction in the angle θ_{15} and a concomitant widening of the angle θ_{24}, or conversely, a SQP distorts toward a TBP by a widening of θ_{15} and a reduction of θ_{24}.

The program managed to embrace all 157 usable five-coordinate entries, thereby indicating that our working angular definition for a pentacoordinate geometry certainly encompassed all those molecular geometries traditionally defined as five-coordinate, at least insofar as nickel, palladium, platinum, rhodium, and iridium were concerned. Moreover, the program managed in almost all cases to label those atoms containing the largest interatomic angle as atoms 1 and 5, and those with the second largest as atoms 2 and 4, respectively, in line with the convention adopted in Table I and Figure 1. Not only does the program therefore offer a means of searching for a five-coordinate fragment but also it has the added advantage of beginning to superimpose onto that fragment a uniform ligand numbering scheme.

Identification of Four-Plus-One Coordinate Entries. A search of the same version of the CSD yielded 624 entries containing nickel in a four-coordinate environment, 428 entries containing palladium, and 656 platinum-, 165 rhodium-, and 69 iridium-containing entries. This database was searched for the presence of six-atom fragments, i.e., four-plus-one coordinate fragments, whose geometry corresponded to that outlined in Table I. A total of 25 hits for the nickel complexes, 22 for palladium, 26 for platinum, 15 for rhodium, and 11 for iridium were obtained. These were sorted along the same criteria as used for the five-coordinate entries, finally yielding 7 nickel, 10 palladium, 1 platinum, 3 rhodium, and 1 iridium entries that could be considered as four-plus-one coordinate.[19]

Table II. Keywords and Parameters Used during the Search for Four-plus-One Coordinate Entries

```
INPUT...FRAG PT 5 CONNECTED
INPUT...C
INPUT...C THIS GEOM RUN ATTEMPTS TO FIT
INPUT...C A GENERAL 5 COORD GEOMETRY TO
INPUT...C THE 5 CONNECTED PT ENTRIES.
INPUT...C
INPUT...C
INPUT...AT1 AA
INPUT...AT2 AA
INPUT...AT3 AA
INPUT...AT4 AA
INPUT...AT5 AA
INPUT...AT6 PT
INPUT...BO 6 1
INPUT...BO 6 2
INPUT...BO 6 3
INPUT...BO 6 4
INPUT...BO 6 5
INPUT...TEST DIST 6 1 1.5 3.4
INPUT...TEST DIST 6 2 1.5 3.4
INPUT...TEST DIST 6 3 1.5 3.4
INPUT...TEST DIST 6 4 1.5 3.4
INPUT...TEST DIST 6 5 1.5 3.4
INPUT...TEST ANG 1 6 5 150 181
INPUT...TEST ANG 2 6 4 105 175
INPUT...TEST ANG 1 6 2 75 108
INPUT...TEST ANG 1 6 4 75 108
INPUT...TEST ANG 1 6 3 80 110
INPUT...TEST ANG 5 6 2 65 107
INPUT...TEST ANG 5 6 4 65 107
INPUT...TEST ANG 5 6 3 65 108
INPUT...TEST ANG 2 6 3 70 132
INPUT...TEST ANG 3 6 4 70 132
INPUT...END
```

Finally, therefore, the total number of entries in the CSD that might be construed as being five-coordinate (or, at least, four-plus-one coordinate) is 104 for nickel, 15 for palladium, 9 for platinum, 25 for rhodium, and 26 for iridium. Of these, six nickel, three rhodium and five iridium entries represent dimeric compounds with two geometrically distinct metal atoms, while one of the nickel hits, being tetrameric, contains four independent and distinct nuclei. This leads to a database containing a total of 196 unique five-coordinate metal centers: 113 with nickel, 15 with palladium, 9 with platinum, 28 with rhodium, and 31 with iridium.[20]

2. Description of Molecular Geometry. The observed molecular geometries are to be referred to idealized TBPs and SQPs, of D_{3h} and C_{4v} symmetry, respectively. In order to accomplish this, three things are necessary. First, a set of coordinates suitable to defining uniquely the structure of each molecular fragment needs to be adopted, and second, a method of describing their distortion away from the reference geometries is needed. Finally, a unique system of nomenclature is required in order to ensure that these coordinates are consistently defined in both the reference geometries and in the observed fragments.

Murray-Rust, Bürgi, and Dunitz[21-23] have described the distortion of an observed structure away from a more symmetrical reference molecule, with the same atomic connectedness or constitution, in terms of a *total displacement (or distortion) vector* $\mathbf{D} = d_j\mathbf{p}_j = [d_j(\text{obs}) - d_j(\text{ref})]\mathbf{p}_j$, where d_j(obs) and d_j(ref) represent the internal parameters of the observed and reference molecules, respectively. That is, d_j reflects the *displacement* of the observed structure along the displacement coordinate $\mathbf{p}_j$. Now, instead of internal coordinates being used to construct the

(14) Berry, R. S. *J. Chem. Phys.* **1960**, *32*, 933–941.
(15) Holmes, R. R. *Prog. Inorg. Chem.* **1984**, *32*, 119–235.
(16) Rossi, A. R.; Hoffmann, R. *Inorg. Chem.* **1975**, *14*, 365–374.
(17) Burdett, J. K. *Adv. Inorg. Chem. Radiochem.* **1978**, *21*, 113–146.
(18) Gillespie, R. J. *J. Chem. Soc.* **1963**, 4679–4685.
(19) A breakdown of these compounds may be obtained on request from the authors.
(20) A list of reference codes, ligand atom types, and interatomic distances and angles may be obtained on request from the authors.
(21) Murray-Rust, P.; Bürgi, H.-B.; Dunitz, J. D. *Acta Crystallogr.* **1978** *B34*, 1787–1793.
(22) Murray-Rust, P.; Bürgi, H.-B.; Dunitz, J. D. *Acta Crystallogr.* **1978**, *B34*, 1793–1803.
(23) Murray-Rust, P.; Bürgi, H.-B.; Dunitz, J. D. *Acta Crystallogr.* **1979**, *A35*, 703–713.

Table III. Symmetry Coordinates of TBP[a]

species A_1'	$S_1 = 2^{-1/2}(r_1 + r_5)$
	$S_2 = 3^{-1/2}(r_2 + r_3 + r_4)$
	$S_{01} = \Delta\theta_{15}$ (R)
	$S_{02} = 3^{-1/2}(\Delta\theta_{24} + \Delta\theta_{23} + \Delta\theta_{34})$ (R)
	$S_{03} = 6^{-1/2}(\Delta\theta_{13} + \Delta\theta_{12} + \Delta\theta_{14} + \Delta\theta_{35} + \Delta\theta_{25} + \Delta\theta_{45})$ (R)
species A_2''	$S_3 = 2^{-1/2}(r_1 - r_5)$
	$S_4 = 6^{-1/2}(\Delta\theta_{12} + \Delta\theta_{13} + \Delta\theta_{14} - \Delta\theta_{25} - \Delta\theta_{35} - \Delta\theta_{45})$
species E'	$S_{5a} = 6^{-1/2}(2r_3 - r_2 - r_4)$
	$S_{5b} = 2^{-1/2}(r_2 - r_4)$
	$S_{6a} = 6^{-1/2}(2\Delta\theta_{24} - \Delta\theta_{34} - \Delta\theta_{23})$
	$S_{6b} = 2^{-1/2}(\Delta\theta_{34} - \Delta\theta_{23})$
	$S_{7a} = 12^{-1/2}(2\Delta\theta_{13} - \Delta\theta_{12} - \Delta\theta_{14} + 2\Delta\theta_{35} - \Delta\theta_{25} - \Delta\theta_{45})$
	$S_{7b} = {}^1/_2(\Delta\theta_{12} - \Delta\theta_{14} + \Delta\theta_{25} - \Delta\theta_{45})$
species E''	$S_{8a} = 12^{-1/2}(2\Delta\theta_{13} - \Delta\theta_{12} - \Delta\theta_{14} - 2\Delta\theta_{35} + \Delta\theta_{25} + \Delta\theta_{45})$
	$S_{8b} = {}^1/_2(\Delta\theta_{12} - \Delta\theta_{14} - \Delta\theta_{25} + \Delta\theta_{45})$

[a] Coordinates marked (R) are considered redundant. Numbering of atoms in TBP is shown in Figure 1.

Table IV. Symmetry Coordinates of SQP[a]

species A_1	$S_1 = r_3$
	$S_2 = {}^1/_2(r_1 + r_2 + r_4 + r_5)$
	$S_3 = 2^{-1/2}(\Delta\theta_{15} + \Delta\theta_{24})$
	$S_{01} = {}^1/_2(\Delta\theta_{13} + \Delta\theta_{23} + \Delta\theta_{34} + \Delta\theta_{35})$ (R)
	$S_{02} = {}^1/_2(\Delta\theta_{12} + \Delta\theta_{14} + \Delta\theta_{25} + \Delta\theta_{45})$ (R)
species B_1	$S_4 = {}^1/_2(r_1 + r_5 - r_2 - r_4)$
	$S_5 = 2^{-1/2}(\Delta\theta_{15} - \Delta\theta_{24})$
	$S_{04} = {}^1/_2(\Delta\theta_{13} + \Delta\theta_{35} - \Delta\theta_{23} - \Delta\theta_{34})$ (R)
species B_2	$S_6 = {}^1/_2(\Delta\theta_{12} + \Delta\theta_{45} - \Delta\theta_{14} - \Delta\theta_{25})$
species E	$S_{7a} = 2^{-1/2}(r_1 - r_5)$
	$S_{7b} = 2^{-1/2}(r_4 - r_2)$
	$S_{8a} = 2^{-1/2}(\Delta\theta_{13} - \Delta\theta_{35})$
	$S_{8b} = 2^{-1/2}(\Delta\theta_{34} - \Delta\theta_{23})$
	$S_{9a} = 2^{-1/2}(\Delta\theta_{12} - \Delta\theta_{45})$
	$S_{9b} = 2^{-1/2}(\Delta\theta_{14} - \Delta\theta_{25})$

[a] Coordinates marked (R) are considered redundant. Numbering of atoms in SQP is shown in Figure 1.

displacement vector, *symmetry-adapted linear combinations of positional or internal coordinates*, also known as *symmetry coordinates*, may just as readily be used. These are linear combinations of the internal coordinates of the molecule, chosen in such a way that they are orthonormal and form bases for irreducible representations of the symmetry group of the molecule. Tables III and IV list sets of symmetry coordinates derived by standard group-theoretical techniques[24,25] for the two reference molecules of D_{3h} (TBP) and C_{4v} (SQP) symmetry, respectively. Note that it is the *difference* (Δ) between the angles of the idealized molecules and the observed ones that appear in the expressions for the symmetry coordinates. Similarily, r_1, r_2, etc. refer to the *deviations* of the observed bond lengths from some standard ones. In practice, however, the actual values of d_i(ref) are important only for the totally symmetric coordinates, since they cancel out for all others.

In all, there are 15 internal coordinates, but only 12 are independent. Redundant (or dependent) coordinates were chosen as follows. First, in the case of the TBP, all three redundancies are of A'_1 symmetry, while for the SQP two are of A_1 and one is of B_1 symmetry. Second, for the TBP, it can be seen that, for infinitesimal angular displacements, the positive and negative deviations from 120 and 90°, respectively, will cancel for S_{02} and S_{03} so that these two symmetry coordinates can be considered redundant. Third, S_{01} may easily be seen to be a function of S_4 and S_7. Fourth, in the case of the SQP the coordinates S_{01} and S_{02} depend on S_3 as well as on each other. The same argument applies to S_5 and S_{04}.

The above symmetry coordinates have been chosen in a self-consistent way; that is, the particular linear combinations of r's and θ's transforming as two-dimensional representations match in pairs. For example, S_{5a} and S_{6a} for the TBP are both transformed into themselves by the same 2-fold axis, C_2, and mirror planes, σ_h and σ_v. However, the above choice is in no way unique, and several other sets of coordinates could have been chosen. As Murray-Rust, Bürgi, and Dunitz have pointed out,[21] "it is immaterial which set of symmetry coordinates is chosen, so the choice should be made according to convenience." The set of coordinates selected for the TBP is the same as that used previously by Hoskins and Lord[26] in their vibrational analysis of the spectra of PF_5 and AsF_5. This is no coincidence, though, since we wished to investigate, among others, the same chemical phenomenon as they did—exchange of axial and equatorial ligands in the TBP via the Berry mechanism involving a SQP intermediate.

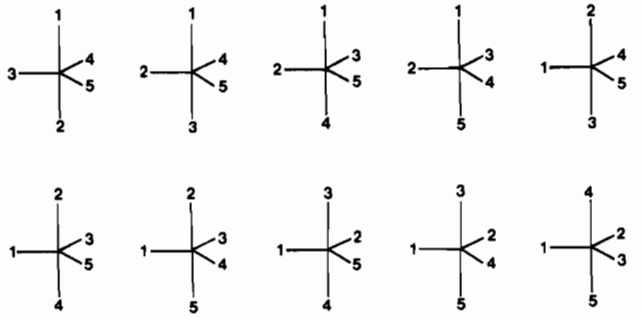

Figure 2. Diagram showing one member (of 12) of each of the 10 groups of distortionally equivalent TBP isomers. The members shown here all have their equatorial ligands numbered ascendingly in a clockwise orientation.

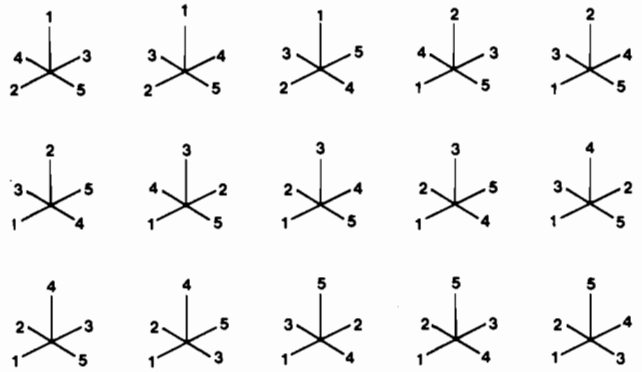

Figure 3. Diagram showing one member (of eight) of each of the 15 groups of distortionally equivalent SQP isomers.

3. Ligand Numbering. In order to relate the observed structures to the two reference geometries via the symmetry coordinates derived above, we need to superimpose the ligand numbering system (used as the basis for the derivation) onto the arrangement of the five ligand atoms about the central metal atom. There are 5! = 120 distinct ways of distributing the five labels (or sites) among these ligands. Some of these would be distinct from each other in the sense that their *absolute* distortion away from either of the reference geometries is different, while others would be related in the sense that their absolute distortion is the same, but the *orientation* of their distortion vectors is different.

Consider, for example, a slightly distorted trigonal-bipyramidal molecule with the following labelings of the ligands:

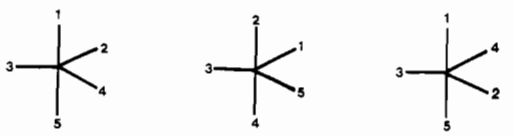

A **B** **C**

The symmetry distortion coordinates for structure A are all close to zero, whereas for structure B they are completely different from zero because the assignment of labels 1 and 5 to equatorial positions implies a significant distortion from the reference structure, in which ligands 1 and 5 are assigned to axial positions. If structures A and C, on the other hand, are compared the symmetry coordinates S_1, S_2, S_3, S_4, S_{5a}, S_{6a}, S_{7a}, and S_{8a} are identical for the two isomers, with S_{5b}, S_{6b}, S_{7b}, and S_{8b} having identical magnitudes but opposite sign for structures A and C,

(24) (a) Wilson, E. B.; Decius, J. C.; Cross, P. C. *Molecular Vibrations—The Theory of Infrared and Raman Vibrational Spectra*; McGraw Hill: London, 1955. (b) Cotton, F. A. *Chemical Applications of Group Theory*; 2nd ed.; Wiley-Interscience: New York, 1971. (c) Wald, D. *Gruppentheorie für Chemiker*, 1. Aufl.; VCH: Weinheim, FRG, Deerfield Beach, FL, 1985.

(25) A detailed derivation of those used in this study may be obtained on request from the authors.

(26) Hoskins, L. C.; Lord, R. C. *J. Chem. Phys.* **1967**, *46*, 2402–2412.

respectively. Thus, the orientations of the distortion vectors of structures A and C in symmetry coordinate space will differ as a result of the different values of the coordinates S_{5b}, S_{6b}, S_{7b}, and S_{8b}. Similar arguments apply to square-pyramidal molecules.

On closer examination of the two examples quoted above the following point emerges. In the case of the TBP permutational isomers that have *the same pair of axial ligands*, but differ in the relative arrangements of their equatorial ligands, will show the same degree of distortion. For the SQP, permutational isomers with *the same apical ligand* will be equally distorted. In fact, for the TBP, it turns out that there are 10 possible ways of combining the five ligands into pairs of axial ligands (the number of permutations divided by the order of the point group; 120/12 = 10). We will call isomers whose absolute displacements from the reference molecule are equal *distortionally equivalent*. For the SQP there are 15 groups of distortionally equivalent isomers (120/8 = 15). Figures 2 and 3 give one example from each of the 10 and 15 groups, respectively, of distortionally equivalent isomers of the TBP and SQP.

We therefore need to label the observed molecules in only 10 or 15 possible ways, depending on whether we are attempting to view them as distorted TBP or distorted SQP, respectively, and then find the labeling that yields the shortest displacement vector for a given observed structure.

In our case, we decided to determine the observed distortion away from the idealized molecules not in the 12-dimensional space spanned by the complete set of symmetry coordinates, but rather in a space of reduced dimensionality defined by the symmetry coordinates composed of bond angle displacements only. The rationale behind this is the following. We are mainly interested in distinguishing whether a given structure is close to the TBP or the SQP; for this decision interatomic distances, and hence symmetry coordinates involving these, are irrelevant. For the TBP, therefore, the observed distortion is estimated by the length of the seven-dimensional displacement vector whose components are the displacement of the observed structures along the coordinates S_4, S_{6a}, S_{6b}, S_{7a}, S_{7b}, S_{8a}, and S_{8b}. Where an observed structure is to be related to a SQP, however, a complication arises in that the trans-basal angles (θ_{15} and θ_{24}) are not fixed by the C_{4v} symmetry of a SQP, but may adopt any value between 0 and 360°—so long as they are identical with each other. For this reason the displacement of the observed structures along the S_3 coordinate cannot be evaluated since there are no values θ_{15}(ref) and θ_{24}(ref) from which the deviations ($\Delta\theta_{15}$ and $\Delta\theta_{24}$) of the observed values can be estimated. (Earlier, it was pointed out that, for all symmetry coordinates apart from the perfectly symmetrical ones, the values of d_j(ref) cancel out—S_3 is of type A_1, though.) Consequently, we decided to estimate the observed distortion by means of a six-dimensional vector whose components are the displacements of the observed structures along the coordinates S_5, S_6, S_{8a}, S_{8b}, S_{9a}, and S_{9b}. Of course, this is by no means a perfect solution, but short of subjectively hypothesizing what the "ideal" trans-basal angle might be, it seems to be the only one.

The procedure for determining that numbering of the five ligands in each individual observed structure which most closely approximates the one used as a basis (Table I and II) may consequently be outlined as follows: (i) determine the length of the displacement vector for the particular permutation of the ligands as it appears originally in the data matrix; (ii) permute this arrangement through all the distortionally *non*equivalent groups and calculate the length of the displacement vector at each stage; (iii) store that permutation which corresponds to the least distortion.

These calculations and permutations were accomplished by means of a FORTRAN program written specifically for these tasks.[27]

4. Expansion of Data Set. The task of labeling the ligands in the observed structures is not complete with the identification of the group of minimally distorted permutation isomers. What the above process has done is to merely identify the pair of axial ligands in a distorted TBP and to fix the apical ligand and the two pairs of trans-basal ligands for a distorted SQP. (Note: We speak of *axial* ligands in the case of a TBP, and of an *apical* ligand when referring to a SQP.) Within each group of distortionally equivalent isomers there are 12 or 8 possible isomeric arrangements of the ligands for the TBP and SQP, respectively. These are related to each other by the symmetry operations of the D_{3h} and C_{4v} point groups. Figures 4 and 5 illustrate this point *highly schematically*, since it must be borne in mind that the 12 and 8 asymmetric units, respectively, containing the distortionally equivalent isomers exist in seven- and six-dimensional space, respectively, and not in two-dimensional space as shown in the figures.

The figures also show how the representative point for an observed structure can be found in either of the 12 or 8 asymmetric units, respectively, of the TBP or SQP parameter space, while being equidistant from the origin in all cases. The origin in Figure 5 ought to be seen not as a point, but rather as a line perpendicular to the plane of the diagram and corresponding to the coordinate S_3, along which the SQP has a degree of freedom.

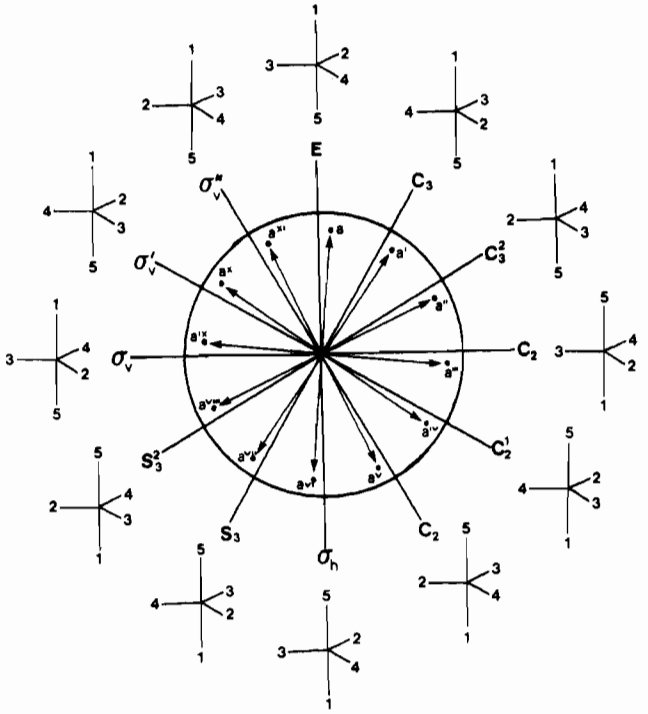

Figure 4. Diagram showing *schematically* how the 12 isometric members of a distortionally equivalent group are generated from the D_{3h} reference structure (=E) and how the representative point for an observed structure may be similarly placed (a, a^{i}, a^{ii}, ...) in either of 12 asymmetric units composing the parameter space, while constantly being equidistant from the origin (see text). Note that the pair of axial ligands is constant.

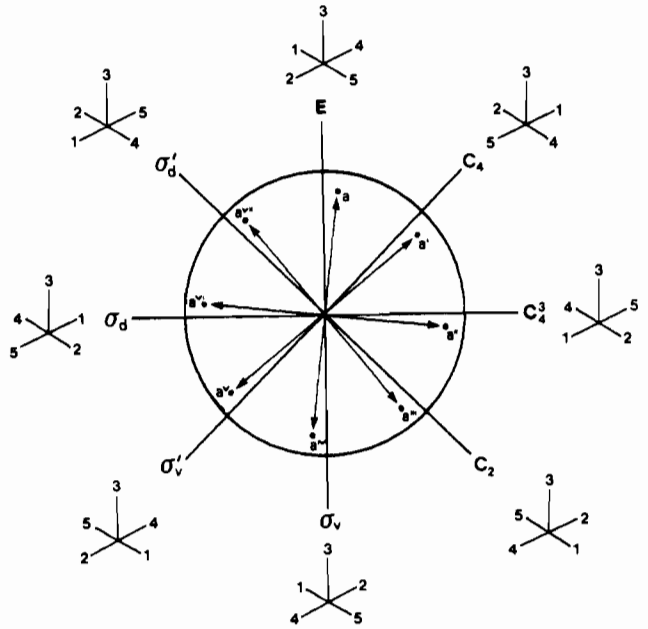

Figure 5. Diagram showing *schematically* how the eight isometric members of a distortionally equivalent group are generated from the C_{4v} reference structure (=E) and how the representative point for an observed structure may be similarly placed in either of the eight asymmetric units composing the parameter space (a, a^{i}, a^{ii}, ...), while constantly being equidistant from the "origin" (see text). Note that the apical ligand is constant as are the pairs of trans-basal angles.

Which of the subspaces in the D_{3h} and C_{4v} parameter spaces the representative point for an observed structure is placed into depends essentially on the order in which the ligands appear originally in the data matrix. The reason for this is that the permutation that appears originally is simply one of either 12 or 8 distortionally equivalent possibilities, and it therefore fixes the particular asymmetric unit within which the

(27) Copies of these programs may be obtained on request from the authors.

permutations outlined above take place. Since the order in which the CSD lists the ligands depends in part on the order in which the original authors listed them, it follows that the starting permutations for the algorithm described above, and thus the representative points for the least distorted TBPs or SQPs, will be randomly distributed among the available subspaces. This has implications for the subsequent statistical analysis of the data point distribution. For example, in the D_{3h} parameter space there are 12 symmetry-related asymmetric units, which would each contain no more than ~16, on average, of the 196 observations in our data set. Clearly this does not make a statistical analysis of the data distribution particularly feasible.

Consequently a unique system of labeling the five ligands must be devised in order to ensure that the representative points are all confined to the same asymmetric unit, rather than being randomly distributed among the 12 or 8 available subspaces, respectively. Murray-Rust has developed an ingenious way of dealing with this problem,[28] which begins with the realization that the symmetry of the reference structure implies a corresponding symmetry of the parameter space.[23]

In our case the 8 or 12 distortionally equivalent isomers in the C_{4v} or D_{3h} parameter spaces, respectively (hereinafter referred to as *S-space*, for square-pyramidal space, and *T-space*, for trigonal-bipyramidal space), are related to each other by the symmetry operations of the respective point groups as shown in Figures 4 and 5. In other words, by starting off with an arbitrary isomer, we may generate its distortionally equivalent siblings by subjecting the original permutation to the symmetry operations of that data space. Similarly, the *complete* data distribution in the 12-dimensional spaces may be obtained by subjecting each of the representative points to the transformation of the symmetry elements. The symmetry in the data distribution that results from this may be profitably utilized in subsequent statistical analyses, since whatever symmetry is present in the data distribution must become evident in the analysis results.

Murray-Rust[28] and Bürgi and Nørskov-Lauritsen[29] have demonstrated how this approach can be used. What it amounts to, in our case, is an expansion of the number of data points by a factor equal to the order of the point groups to which we are referring the observed structure. Thus, if the compounds are to be referred to the TBP, the number of data points is multiplied by 12 (one for each of the 12 operations of the group) while in the case of the SQP the factor is 8. Consequently we end up with 2352 (=12 × 196) and 1568 (=8 × 196) data points in T- and S-space, respectively! It must be emphasized here that this data expansion only brings into prominence the symmetry structure already present in the data base; it does not add new data.

The expansion of the permuted data set put out by the algorithm described above was accomplished by a FORTRAN program written specifically for this purpose.[27]

5. Scaling and Standardization. (a) Standard Bond Lengths. Our data set not only contains a mixture of interatomic distances and angles but also mixes atoms of different kinds, i.e., bonds not of the same *type*. Thus it contains bonds between nickel and oxygen, palladium and iodine, platinum and tin, etc. Both of these factors can be expected to have considerable impact on any statistical analysis we might attempt; for this reason, we need to intelligently standardize and/or scale the data prior to any such analysis.

The first problem is to put all the interatomic distances on a common scale. This is important since we want to be able to compare nickel complexes with those of, e.g., platinum. Futhermore, we need to have some measure of "standard" bond lengths, from which the deviations in the observed structures can be calculated in order that we may obtain values for the totally symmetric coordinates S_1 and S_2 in both D_{3h} and C_{4v} parameter space. By "standard" bond length is meant some empirically obtained value for the average distance (in some statistical sense) between a given pair of atoms.

Klebe and Bürgi[30] have examined two different empirical bond strength (n)–bond length (d) relationships and have found that "standard" distances between a given pair of atoms derived from the two expressions were the same (within three standard deviations) in 15 of 18 cases. The two empirical models were those of Pauling (eq I) and of Brown and Shannon (eq II).[31,32] These relate the standard (d_{i0}) and the observed (d_i) values for the ith type of bond to their respective empirical bond strengths n_0 and n_i. The data set used in that study consisted of four-, five-, and six-coordinated Mg, Al, Si, and P compounds and values of d_{i0}, c, and N (both empirical constants) were determined by minimizing the expression

$$n_i/n_0 = \exp[-(d_i/d_{i0})/c] \quad \text{(I)}$$

$$n_i/n_0 = (d_i/d_{i0})^{-N} \quad \text{(II)}$$

$$(\mathrm{CN}_0 - \sum_{i=1}^{\mathrm{CN}} n_i)^2 \quad \text{(III)}$$

separately for different ligand atoms, but considering all coordination numbers (CN) simultaneously; CN_0 is a reference coordination number and n_0 is taken as 1.

We have proceeded similarily, employing the program written by Klebe and Bürgi, and have obtained values for standard bond lengths between the various metals and their ligand donor atoms for a reference coordination number of five. The results are presented in Table V. The input data consisted of the set of five-coordinate complexes extracted from the CSD as explained earlier, as well as the four-coordinate CSD entries for each type of metal as at July 1984. Just as in the previous study, we see that almost invariably the results obtained from expression I (a) are within three standard deviations of those from II (b), although in some cases this means little, since the standard deviations are large.

In general, the results obtained for the nickel, palladium, platinum, and rhodium data sets are good as judged by the standard deviations, these being less than 0.05 Å in many cases. Moreover, in the majority of cases, the standard deviations for the reference bond lengths obtained from II are smaller than those from I, most noticeably so in the case of the iridium complexes. Here the large σ^2 values result from the way in which the different types of ligand atoms are combined in the complexes composing the data set; the four-coordinate iridium complexes, for example, contain only carbon and phosphorus ligands. As a consequence of this, the algorithm cannot establish a reference value for, e.g., a bond to bromine, since it needs to have this type of bond appear in both four- and five-coordination in order to minimize expression III over various values of CN.

Also listed in Table V are values for standard bond lengths obtained from Pauling.[31] These empirical values may well be somewhat dated, but they still generally fall into or slightly below the range of values that we have found. The fact that many of Pauling's standard bond lengths are lower than ours may nonetheless be significant, insofar as his often pertain to four-coordinate complexes especially in the case of platinum and palladium, while ours have been derived for five-coordination. For the sake of comparison, we have also included in Table V standard bond lengths obtained from expression I for a reference coordination number of four.

It may be seen that for palladium and platinum our reference values for $\mathrm{CN}_0 = 4$ are generally well within 3 standard deviations of Pauling's, while for nickel and rhodium they are on the whole slightly smaller. These observations support the suggestion made above. The almost nonsensical values obtained for the standard bond lengths for four-coordinate iridium are the result of the same problem that plagued the derivation of these values for the five-coordinate metal from equation I—an insufficient dataset.

In the light of the overall better results obtained from eq II, we decided to use these as our reference bond lengths, i.e., as the standard bond length between a given pair of atoms in a five-coordinate complex, to which the observed interatomic distances would be related.

(b) Scaling and Angle Measurements. The description of the geometry of the observed structures involves the use of both linear and angular displacement coordinates. Consequently there is a mixture of variables of considerably different magnitudes: angstroms and degrees. Obviously, the larger the magnitude and/or variation of a given variable, the greater its relative influence on the statistical analysis and the more skewed the results potentially become. In order to overcome this problem, it is often good practice to scale the variables.

In our case, we decided to express the angular displacements in radians related to a circle of a radius r whose length equals the *average* metal-to-ligand distance in the data set. In other words, an angle θ measured in degrees would then correspond to a radial displacement α measured in angstroms according to

$$\alpha = 2\pi r(\theta/360°)$$

We obtained a mean r of 2.231 Å from the average values for the data set, of the bond lengths d_1 = 2.226 Å, d_2 = 2.227 Å, d_3 = 2.388 Å, d_4 = 2.152 Å, and d_5 = 2.161 Å referred, respectively, to a SQP. The exact value of r is not of extreme importance so long as it is reasonably rep-

(28) Murray-Rust, P. *Acta Crystallogr.* **1982**, *B38*, 2765–2771.
(29) Nørskov-Lauritsen, L.; Bürgi, H.-B. *J. Comput. Chem.* **1985**, *6*, 216–228.
(30) Klebe, G.; Bürgi, H.-B. Presented at the 13th International Congress and General Assembly, IUCR, Hamburg, FRG, 1984; Abstr. No. 04.1-7.
(31) Pauling, L. *The Nature of the Chemical Bond*; Cornell University Press; Ithaca, NY, 1940.
(32) Brown, I. D.; Shannon, R. D. *Acta Crystallogr.* **1973**, *A29*, 266–282.

Table V. Standard Bond Lengths d_{i0} and Standard Deviations (in Parentheses) for Five-Coordinate Metal Complexes[a]

	result set	Ni	Pd	Pt	Rh	Ir
H	a	1.469 (325)			1.262 (390)	0.951 (1758)
	b	1.370 (296)			1.478 (113)	1.633 (210)
	c	1.51			1.62	1.62
	d	1.233 (325)			1.098 (390)	0.314 (1758)
C	a	1.958 (30)		2.193 (43)	2.100 (28)	1.925 (664)
	b	1.895 (30)		1.892 (112)	2.077 (29)	1.988 (29)
	c	1.98		2.08	2.09	2.09
	d	1.722 (30)		1.989 (43)	1.937 (28)	1.287 (664)
N	a	2.067 (14)	2.166 (10)	2.221 (11)	2.121 (43)	1.996 (626)
	b	2.068 (13)	2.263 (18)	2.231 (50)	2.024 (30)	1.910 (79)
	c	1.91	2.01	2.01	2.02	2.02
	d	1.831 (14)	2.007 (10)	2.017 (11)	1.957 (43)	1.357 (626)
O	a	2.038 (27)	2.132 (13)		2.189 (52)	
	b	2.028 (32)	2.180 (26)		2.165 (48)	
	c	1.87	1.97		1.98	
	d	1.802 (27)	1.974 (13)		2.026 (52)	
P	a	2.236 (26)	2.407 (23)	2.502 (38)	2.333 (50)	2.568 (392)
	b	2.271 (17)	2.394 (38)	2.531 (144)	2.307 (20)	2.347 (27)
	c	2.31	2.41	2.41	2.42	2.42
	d	2.000 (26)	2.249 (23)	2.297 (38)	2.169 (50)	1.930 (392)
S	a	2.365 (16)	2.478 (13)	2.480 (25)	2.445 (77)	2.310 (656)
	b	2.333 (19)	2.667 (73)	2.243 (158)	2.339 (54)	2.339 (42)
	c	2.25	2.35	2.35	2.36	2.36
	d	2.129 (16)	2.320 (13)	2.276 (25)	2.281 (77)	1.672 (656)
Cl	a	2.348 (43)	2.489 (14)	2.497 (16)	2.399 (84)	2.127 (1076)
	b	2.351 (35)	2.513 (78)	2.639 (230)	2.383 (49)	2.483 (98)
	c	2.20	2.30	2.30	2.31	2.31
	d	2.112 (43)	2.331 (14)	2.293 (16)	2.235 (84)	1.489 (1076)
Ge	a			2.420 (64)		
	b			2.421 (22)		
	c			2.53		
	d			2.216 (64)		
As	a	2.445 (50)	2.419 (41)			
	b	2.472 (43)	2.448 (40)			
	c	2.42	2.52			
	d	2.181 (50)	2.261 (41)			
Br	a	2.437 (52)	2.558 (34)	2.497 (97)	2.455 (187)	2.264 (1450)
	b	2.410 (44)	2.645 (58)	2.458 (220)	2.538 (69)	2.628 (204)
	c	2.35	2.45	2.45	2.46	2.46
	d	2.201 (52)	2.400 (34)	2.292 (97)	2.292 (187)	1.626 (1450)
Sn	a	2.688 (188)		2.565 (60)		
	b	2.597 (212)		2.564 (22)		
	c	2.61		2.71		
	d	2.45 (188)		2.361 (60)		
Sb	a				2.432 (217)	
	b				2.490 (73)	
	c				2.73	
	d				2.267 (217)	
I	a	2.507 (75)	2.731 (49)		2.208 (505)	2.302 (1096)
	b	2.546 (54)	2.806 (53)		2.619 (129)	2.636 (116)
	c	2.54	2.64		2.65	2.65
	d	2.243 (75)	2.573 (49)		2.044 (505)	1.664 (1096)
m		690	211	245	235	171
N_{obs}		145	49	59	52	35

[a] (a) Results for expression I; (b) results for expression II; (c) values taken from Pauling;[31] (d) results for expression I with $CN_0 = 4$; m = number of distances used in refinement; N_{obs} = number of structures in data set.

resentative of the distances that appear in the data. As a consequence of this scaling, a change in a given angle of 10°, for example, would correspond to a radial displacement of 0.390 Å—a value much closer to the distances or bond distance increments typical of the data set than the original angular displacement.

Results and Discussion

1. Univariate Statistics. The variances of the individual symmetry coordinates offer some interesting but limited insights into the underlying distortions of the ML_5 fragment. Table VI gives the standard deviation and variance of each symmetry coordinate in T-space, as well as the percentage of the total variance in the linear and angular symmetry coordinates, respectively, which each can account for. Table VII gives the same information for the data distribution in S-space.

In the interpretation of these results, we shall make use of the graphical representation of symmetry coordinates, a technique in common use in standard texts on vibrational analysis.[24] This involves representing the degrees of freedom of the internal coordinates in a symmetry coordinate by appropriate arrows on a diagram of the molecular fragment. Usually these arrows are drawn in a length proportional to the coefficient of the internal coordinate in the symmetry coordinate, but in our case we chose to represent the degrees of freedom by singly or doubly headed arrows, instead, since the coefficients in our case are always either

Table VI. Standard Deviations (σ), Variances (σ^2), Percentage of Variance in Linear Symmetry Coordinates (% LV), and Percentage of Variance in Angular Coordinates (% AV) for T-Space Data Distribution

	σ, Å	σ^2, Å^2	% LV	% AV
S_1	0.171	0.029	15.0	
S_2	0.134	0.018	9.2	
S_3	0.133	0.018	9.2	
S_4	0.358	0.128		3.6
S_{5a}	0.254	0.065	33.3	
S_{5b}	0.254	0.065	33.3	
S_{6a}	1.236	1.529		44.4
S_{6b}	1.236	1.529		44.4
S_{7a}	0.233	0.054		1.6
S_{7b}	0.233	0.054		1.6
S_{8a}	0.272	0.074		2.2
S_{8b}	0.272	0.074		2.2

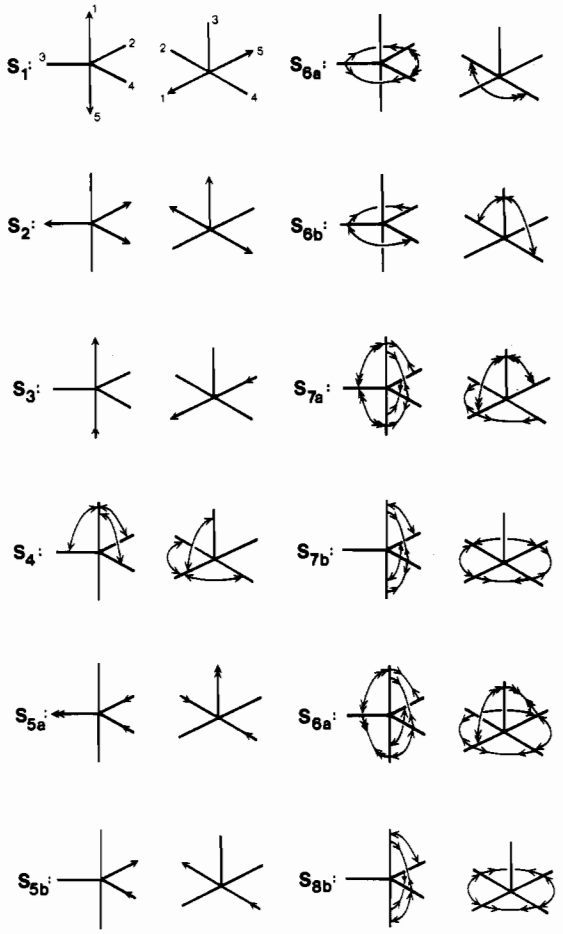

Figure 6. Graphic representation of D_{3h} symmetry coordinates referred to a TBP and a SQP.[33] Single-headed arrows indicate changes in internal coordinates whose coefficient in the symmetry coordinate is 1; double-headed arrows represent those with a coefficient of 2. Only *independent* distortions are shown.

1 or 2. Figure 6 graphically illustrates the D_{3h} symmetry coordinates referred to both a TBP and a SQP.[33] Only *independent* distortions are shown, i.e. those that do not follow naturally from others. For example, in S_4 ($= 6^{-1/2}(\theta_{12} + \theta_{13} + \theta_{14} - \theta_{25} - \theta_{35} - \theta_{45})$) the decrease in the angles *below* the equatorial plane perforce results from the simultaneous increase of all three *above* the plane. Consequently, only the latter are detailed for S_4 in Figure 6. The C_{4v} symmetry coordinates are graphically illustrated in Figure 7, referred to both a SQP and a TBP.[34]

(33) This is done to facilitate the interpretation of data relating to both TBPs and SQPs that might exist in T-space, a point which will become clear in due course.
(34) This is done for similar reasons, as before.

Table VII. Standard Deviations (σ), Variances (σ^2), Percentage of Variance in Linear Symmetry Coordinates (% LV), and Percentage of Variance in Angular Symmetry Coordinates (% AV) for S-Space Data Distribution

	σ, Å	σ^2, Å^2	% LV	% AV
S_1	0.317	0.101	59.8	
S_2	0.177	0.031	18.6	
S_3	0.492	0.242		18.0
S_4	0.109	0.012	7.2	
S_5	0.801	0.642		47.6
S_6	0.268	0.072		5.4
S_{7a}	0.110	0.012	7.2	
S_{7b}	0.110	0.012	7.2	
S_{8a}	0.361	0.131		9.7
S_{8b}	0.361	0.131		9.7
S_{9a}	0.253	0.064		4.8
S_{9b}	0.253	0.064		4.8

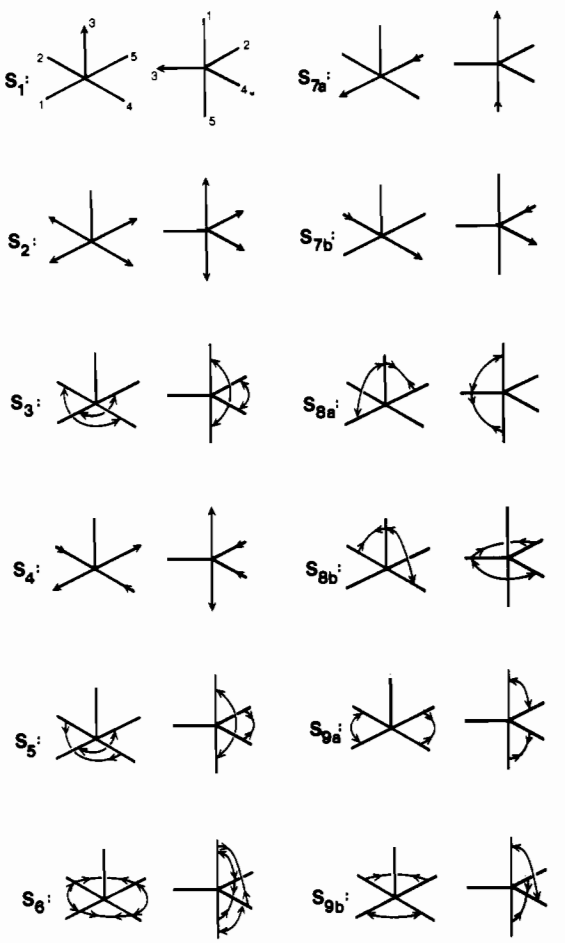

Figure 7. Graphic representation of C_{4v} symmetry coordinates referred to a SQP and a TBP.[34] Single-headed arrows indicate changes in internal coordinates whose coefficient in the symmetry coordinate is 1; double-headed arrows represent those with a coefficient of 2. Only *independent* distortions are shown. See also footnote *b* in Table IX.

Considering first the variance in the bond increment (linear) symmetry coordinates for the TBP, a comparison of Table VI with Figure 6 reveals that there is a fair amount of variance in the lengths of the axial bonds (S_1) but an even greater one in those of the equatorial bonds (S_{5a}), with two of the bonds becoming shorter as the third lengthens, or vice versa. Possibly related to this is the variance in the bond angle (angular) symmetry coordinates of S_{6a} and S_{6b}, the largest by far, with S_{6a} indicating that there is a large variance in the equatorial angles, with one opening up while the other two become smaller, or vice versa. For S-space, the largest contribution to the bond increment symmetry coordinates comes from S_1, which suggests that there is a large variance in the apical distance of the SQP. For the bond angle symmetry coordinates, the largest contribution comes from S_5, indicating

Table VIII. Correlation Matrix for Symmetry Coordinates in T-Space[a]

	A_1'		A_2''		E′						E″	
	S_1	S_2	S_3	S_4	S_{5a}	S_{5b}	S_{6a}	S_{6b}	S_{7a}	S_{7b}	S_{8a}	S_{8b}
S_1	1.00											
S_2	−0.55	1.00										
S_3	0.00	0.00	1.00									
S_4	0.00	0.00	−0.67	1.00								
S_{5a}	0.00	0.00	0.00	0.00	1.00							
S_{5b}	0.00	0.00	0.00	0.00	0.00	1.00						
S_{6a}	0.00	0.00	0.00	0.00	0.59	0.00	1.00					
S_{6b}	0.00	0.00	0.00	0.00	0.00	0.59	0.00	1.00				
S_{7a}	0.00	0.00	0.00	0.00	−0.01	0.00	0.45	0.00	1.00			
S_{7b}	0.00	0.00	0.00	0.00	0.00	−0.01	0.00	0.45	0.00	1.00		
S_{8a}	0.00	0.00	0.00	0.00	0.00	0.00	0.00	0.00	0.00	0.00	1.00	
S_{8b}	0.00	0.00	0.00	0.00	0.00	0.00	0.00	0.00	0.00	0.00	0.00	0.00

[a] Symmetry species to which the coordinates belong are also shown.

Table IX. Correlation Matrix for Symmetry Coordinates in S-Space[a]

	A_1			B_1		B_2	E[b]					
	S_1	S_2	S_3	S_4	S_5	S_6	S_{7a}	S_{7b}	S_{8a}	S_{8b}	S_{9a}	S_{9b}
S_1	1.00											
S_2	−0.78	1.00										
S_3	0.55	−0.48	1.00									
S_4	0.00	0.00	0.00	1.00								
S_5	0.00	0.00	0.00	0.39	1.00							
S_6	0.00	0.00	0.00	0.00	0.00	1.00						
S_{7a}	0.00	0.00	0.00	0.00	0.00	0.00	1.00					
S_{7b}	0.00	0.00	0.00	0.00	0.00	0.00	0.00	1.00				
S_{8a}	0.00	0.00	0.00	0.00	0.00	0.00	−0.27	0.00	1.00			
S_{8b}	0.00	0.00	0.00	0.00	0.00	−0.01	0.00	−0.27	0.00	1.00		
S_{9a}	0.00	0.00	0.00	0.00	0.00	0.00	−0.37	0.37	0.08	−0.08	1.00	
S_{8b}	0.00	0.00	0.00	0.00	0.00	0.00	−0.37	−0.37	0.08	0.08	0.00	1.00

[a] Symmetry species to which the coordinates belong are also shown. [b] The choice of degenerate symmetry coordinates S_7, S_8, and S_9 was not entirely consistent. S_7 and S_8 show mirror planes passing through the apical and two trans-basal bonds. S_9 shows mirror planes including the apical bond and bisecting cis-basal bonds. This does not affect our conclusions, however.

a large variance in the trans-basal angles, with one angle opening up as the other closes.

2. Bivariate Statistics. The correlations between the symmetry coordinates can shed light on a number of things. Recall that they are orthonormal and transform according to the irreducible representations of the point group. It follows, therefore, that symmetry coordinates belonging to different symmetry species should ideally be uncorrelated. This implication may be used to test, first, whether the coordinates that we have derived do in fact form bases for the irreducible representations and, second, whether our manipulations of the data set exchanged parameters that ought not to have been interchanged with each other.

Tables VIII and IX give the correlation matrices for the symmetry coordinates in T-space and S-space, respectively. From these it may be seen quite clearly that symmetry coordinates from different symmetry species (see Tables III and IV) are at least linearly uncorrelated, while those of one symmetry are correlated, often quite highly. In T-space, for example, S_1 and S_2 both belonging to the A_1' representation, have a correlation of −0.55, while they are uncorrelated with any other symmetry coordinates (all of which belong to a different species). Similarly, in S-space the coordinates S_1, S_2, and S_3 (all A_1) are highly correlated, while they are linearly uncorrelated with any others, all of which are of different symmetry.

We may therefore conclude that for the data set *as a whole* the symmetry coordinates which we have chose are not linearly correlated across different symmetry species, either in T- or in S-space. Furthermore, we may see that the routines written to handle the data expansion according to the symmetry operations of the two point groups have operated correctly.

Of more interest, though, is an investigation of the particular distortions that pairs of correlated symmetry coordinates represent. For example, in T-space S_3 ($=2^{-1/2}(r_1 - r_5)$) represents the lengthening of one axial bond (r_1) and a shortening of the other (r_5), while S_4 ($=6^{-1/2}(\theta_{12} + \theta_{13} + \theta_{14} - \theta_{25} - \theta_{35} - \theta_{45})$) is indicative of an "umbrella" type distortion of the TBP whereby the axial–equatorial angles *above* the equatorial plane are increasing, while those *below* are decreasing. In this case, however, because of the negative correlation between S_3 and S_4 ($r = -0.67$) the umbrella distortion is reversed. The *combination* of the two distortions, which are shown in Figure 8, is reminiscent of a classical S_N2 coordinate, i.e. a bimolecular nucleophilic substitution reaction at a tetrahedral center. Another correlation of interest is that between S_{5a} and S_{6a} ($r = 0.59$). These distortions, also represented in Figure 8, mirror part of the Berry intramolecular exchange coordinate along which one of the equatorial ligands (atom 3 in our case) acts as a pivot for the distortion, its distance (r_3) to the metal increasing, while the other two equatorial ligands move

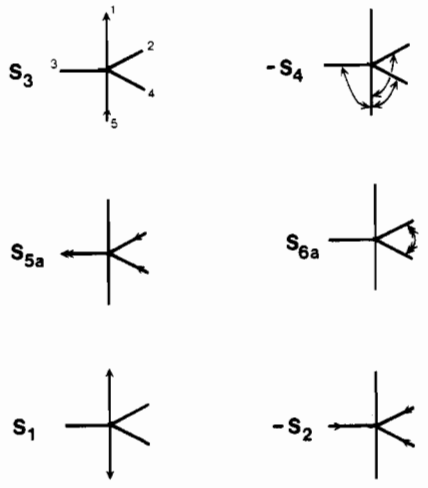

Figure 8. Distortions corresponding to some pairs of correlated symmetry coordinates in T-space. Where the correlation is negative, the inverse of one of the symmetry coordinates is represented, e.g. $-S_4$. It is argued that the *correlated distortions* correspond to (1) the S_N2 coordinate, (2) the Berry coordinate, and (3) the "constant amount of glue" coordinate.

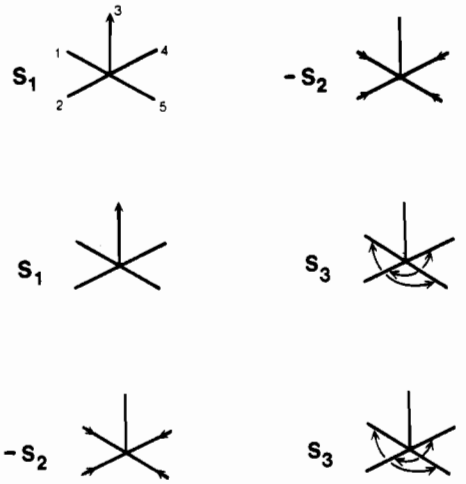

Figure 9. Distortions corresponding to some pairs of correlated symmetry coordinates in S-space. Where the correlation is negative, the inverse of one of the symmetry coordinates is represented, e.g. $-S_2$. It is argued that the *sum* of the *correlated distortions* corresponds to a reversible association coordinate for a square-planar center.

closer towards the metal. Concomitantly they move further apart from each other, increasing the angle between them (θ_{24}) while decreasing the other two equatorial–equatorial angles (θ_{23} and θ_{34}). The last correlation in T-space on which we shall focus is that between S_1 and S_2 ($r = -0.55$); its corresponding distortions are also shown in Figure 8. Here it can be seen that increases in the axial distances (r_1 and r_5) bring about decreases in the equatorial distances (r_2, r_3, r_4), as if there were only a fixed amount of "bonding power" to the metal, this being apportioned equally between the five ligands—if one (or two) are removed this leaves more "glue" for the others, which consequently bond more firmly.[35]

(35) This phenomenon whereby there appears to be a constant amount of bonding associated with the metal atom is reminiscent of Pauling's constant bond order concept, according to which the sum of the bond orders around a given atom stays conserved even as it forms or breaks bonds to other atoms: Pauling, L. *The Nature of the Chemical Bond*; Cornell University Press: Ithaca, NY, 1960. We have chosen to term this coordinate the "constant amount of glue" coordinate as a play on the German work "Klebe"; G. Klebe wrote the program for the determination of standard bond lengths (Section 5(a)) based on this concept of constant bond order, and "Klebe" also means "glue".

In S-space there are only three major correlations. The first, between S_1 ($=r_3$) and S_2 ($=^1/_2(r_1 + r_2 + r_4 + r_5)$), is by far the most important ($r = -0.78$) and represents essentially the S-space equivalent of that between S_1 and S_2 in T-space—the "constant-amount-of-glue" distortion. The second, between S_1 and S_3 ($r = 0.55$), indicates that an increase in the apical distance is correlated with an increase in the trans-basal angles of the SQP, i.e. a flattening of the SQP. The third, between S_2 and S_3 ($r = -0.48$), shows that the flattening of the SQP (S_3) is correlated with a shortening of the metal–basal ligand bond distances. Taken together, the three distortions mirror those of a classical reversible association reaction of a square-planar center. They are illustrated in Figure 9. Finally, the data also exhibit a small distortion along the equivalent of the Berry coordinate in S-space. The correlation ($r = 0.39$) between S_4 and S_5 represents a part of the Berry distortion coordinate, although in this case it accounts for only 15% of the data variance.

One final point of interest is the amount of variance that each pair of variables can maximally describe. This may be judged from the square of the correlation coefficient. From an inspection of the correlation matrix (Table VIII), it can be seen that in the case of T-space the linear relatedness of any two symmetry coordinates can maximally account for 45% of the sample variance (S_3 and S_4), while for S-space (Table IX) the figure is 61% (S_1 and S_2).

3. Summary. The coordination geometry of ML_5 molecular fragments has been analyzed in terms of symmetry displacement coordinates pertaining to a TBP and a SQP. Univariate and bivariate statistics of these coordinates show patterns that are reminiscent of the structural distortions accompanying dissociation of an axial ligand in a TBP or of the apical ligand in a SQP or accompanying a Berry intramolecular exchange.

In the following paper, the distribution of the data in distortion space will be analyzed in finer detail by using methods of cluster analysis. This will lead to a more detailed description of the observed distortions and their relation to chemical reactivity.

Acknowledgment. We thank Dr. Leif Nørskov for help with the data retrieval and Dr. Gerhard Klebe for the use of his computer program for the calculation of standard bond lengths. Professor Luigi Nassimbeni kindly read part of the manuscript for this paper and made valuable comments. The University of the Western Cape granted study leave and financial assistance to T.A.d.H. This work was also supported by the "Schweizerischer Nationalfonds zur Förderung wissenschaftlicher Forschung".